AD

TECHNICAL REPORT ARCCB-TR-97006

DESIGN OF PASSIVE VIBRATION ABSORBER TO REDUCE TERRAIN-INDUCED GUN BARREL VIBRATION IN THE FREQUENCY DOMAIN

ERIC L. KATHE

FEBRUARY 1997

US ARMY ARMAMENT RESEARCH,
DEVELOPMENT AND ENGINEERING CENTER
CLOSE COMBAT ARMAMENTS CENTER
BENÉT LABORATORIES
WATERVLIET, N.Y. 12189-4050

DISCLAIMER

The findings in this report are not to be construed as an official Department of the Army position unless so designated by other authorized documents.

The use of trade name(s) and/or manufacturer(s) does not constitute an official indorsement or approval.

DESTRUCTION NOTICE

For classified documents, follow the procedures in DoD 5200.22-M, Industrial Security Manual, Section II-19 or DoD 5200.1-R, Information Security Program Regulation, Chapter IX.

For unclassified, limited documents, destroy by any method that will prevent disclosure of contents or reconstruction of the document.

For unclassified, unlimited documents, destroy when the report is no longer needed. Do not return it to the originator.

REPORT DOCUMENTATION PAGE

Form Approved
OMB No. 0704-0188

1. AGENCY USE ONLY (Leave blank)	2. REPORT DATE	3. REPORT TYPE AND DATES COVERED
	February 1997	Final

4. TITLE AND SUBTITLE
DESIGN OF PASSIVE VIBRATION ABSORBER TO REDUCE TERRAIN-INDUCED GUN BARREL VIBRATION IN THE FREQUENCY DOMAIN

5. FUNDING NUMBERS
AMCMS No. 6226.24.H180.0
PRON No. 4A6C6FYA1ABJ

6. AUTHOR(S)
Eric L. Kathe

7. PERFORMING ORGANIZATION NAME(S) AND ADDRESS(ES)
U.S. Army ARDEC
Benet Laboratories, AMSTA-AR-CCB-O
Watervliet, NY 12189-4050

8. PERFORMING ORGANIZATION REPORT NUMBER
ARCCB-TR-97006

9. SPONSORING / MONITORING AGENCY NAME(S) AND ADDRESS(ES)
U.S. Army ARDEC
Close Combat Armaments Center
Picatinny Arsenal, NJ 07806-5000

10. SPONSORING / MONITORING AGENCY REPORT NUMBER

11. SUPPLEMENTARY NOTES
Presented at the 8th U.S. Army Gun Dynamics Symposium, Newport, RI, 14-16 May 1996.
Published in proceedings of the symposium.

12a. DISTRIBUTION / AVAILABILITY STATEMENT
Approved for public release; distribution unlimited.

12b. DISTRIBUTION CODE

13. ABSTRACT *(Maximum 200 words)*

This paper presents an applied method for the optimal design of passive vibration absorbers to reduce terrain-induced vibrations of tank cannons. The method uses a finite element model of the cannon, which was formulated using the Euler-Bernoulli transverse beam approximation. This model is then transformed to the Laplace "*s*" domain (transfer function form) using the MATLAB® software package. The design is optimized by assigning a scalar cost function to the frequency response of the modified barrel, which provides a metric for minimizing the design parameter space. The results indicate that the peak amplitude of the frequency response of a 1,500 Kg barrel may be cut in half by an appropriately tuned 20 Kg absorber located at the muzzle. Also, sensitivity of the design to parametric variation and modeling uncertainty is significantly reduced with Rayleigh stiffness proportional damping of the absorber in the range 0.02 $\frac{\text{N/(m/s)}}{\text{N/m}}$.

14. SUBJECT TERMS	15. NUMBER OF PAGES
Finite Element Method, Vibration Absorber, Passive, Design, Cannon	20
	16. PRICE CODE

17. SECURITY CLASSIFICATION OF REPORT	18. SECURITY CLASSIFICATION OF THIS PAGE	19. SECURITY CLASSIFICATION OF ABSTRACT	20. LIMITATION OF ABSTRACT
UNCLASSIFIED	UNCLASSIFIED	UNCLASSIFIED	UL

TABLE OF CONTENTS

LIST OF FIGURES

ACKNOWLEDGMENTS

The author would like to thank Dr. Andrew Lemnios, Rensselaer Polytechnic Institute, Troy, NY, and Dr. Ronald Gast, Dr. Ronald Racicot, and Dr. Patrick Vottis, U.S. Army, Benet Laboratories, Watervliet Arsenal, NY, for their assistance and insightful suggestions.

INTRODUCTION

This paper describes an applied method to optimize the design of passive vibration absorbers to reduce terrain-induced vibrations of tank cannons. The method should improve the accuracy of the weapon by reducing variations in the initial conditions of the gun barrel at shot start.

Applying vibration absorbers to beams involves coupling a damped mass-spring system to the beam at the locations of greatest vibration activity. (Vibration absorbers [1] are also commonly referred to as dynamic dampers [2], vibration neutralizers [3], and tuned-mass-dampers, (TMDs)[4,5].)† This achieves two main benefits. First, the addition of the absorber may reduce the receptance of the modified beam to certain frequency bands of a disturbance force—effectively *rejecting* the disturbance energy. Second, the absorber enhances the dissipation of vibrational energy via the damping of the absorber. This may play a significant role if the damping of the unmodified structure is limited and sustained external excitement is expected, but it generally has less impact on the design. In addition, absorbers may increase receptance at certain frequency bands—an undesirable possibility.

The method presented in this paper uses a Euler-Bernoulli finite element technique to generate the second-order equations of motion of the gun barrel as a non-uniform beam—with subsequent conversion to the first-order state-space domain. [6] This model is then transformed to the Laplace "*s*" domain (transfer function form) using the MATLAB®‡ software package. [7,8,9] In this domain, Bode analysis reveals the frequency response of the system. The design is optimized by assigning a scalar cost function to the frequency response function of the modified barrel, which provides a metric for minimizing the design parameter space of the vibration absorber. This applied approach to the effective design of vibration absorbers forms a middle ground between mere numerical simulation and analytic formulation of the problem.

This paper documents the detailed development of the dynamic modeling and the design of vibration absorbers for application to the XM291 gun system as an elastic beam. All explicit MATLAB® functions and previously written m-files are enclosed by angle brackets to distinguish them from regular text.

THE DYNAMIC MODEL

This report leverages the software developments of a previous effort [6] to formulate the dynamic model of the gun system.

The Barrel

The finite element method was chosen to dynamically model the barrel. This application uses the Euler-Bernoulli beam approximation and Hermite-cubic interpolation functions to form the inertial and stiffness matrices of the undamped second-order equations of motion. This is achieved by approximating

---

† In many engineering contexts, these terms may become misnomers and create confusion.[3] The design of such mechanisms may emphasize dissipation of energy via damping or redistribution of energy within the frequency spectrum. For this application, the absorption of energy into other frequency bands and the dissipation of energy by the damping element are both suspended by the *rejection* of the energy effected by reshaping the frequency response function.

‡ Registered trademark of The MathWorks, Inc., 24 Prime Park Way, Natick, MA 01760-1500.

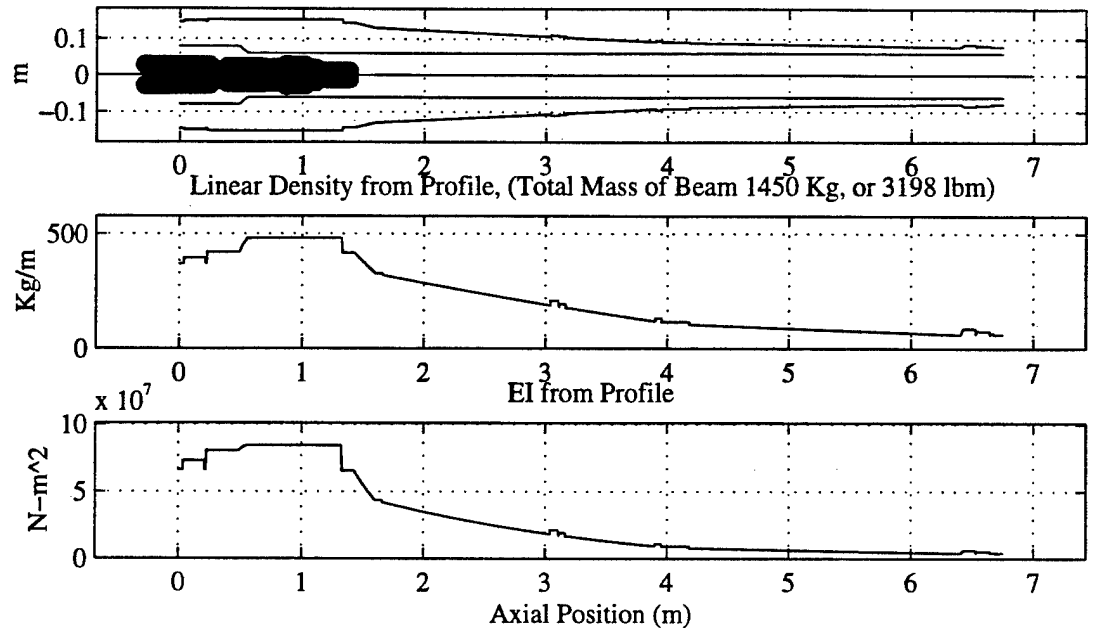

Figure 1. XM291 geometry and material properties data

the continuous non-uniform beam as an assemblage of a finite number of discrete elements. Within each discrete element, the interpolation functions are used to approximate the interior deformation. At the boundary between two adjacent elements, called a node, continuity of lateral displacement and slope is imposed. When assembled, the resulting finite element model dynamics—governed solely by the node states—closely approximate the dynamics of the non-uniform beam.

The geometry and material properties data for the XM291 are read in by the m-file <geomf_XM291.m> [6] and are shown in Figure 1. The upper plot depicts the inner and outer radii of the barrel with respect to the axial position. Within the confines of the inner diameter of the barrel, the distribution of the extraneous mass of components attached to the barrel is shown. The plot reveals that the barrel is configured with its breech and mount hardware—but not with the thermal shrouds, bore evacuator, or muzzle reference mount. For clarification, the title lists the total mass of the extraneous attached hardware. The middle plot indicates the linear density of the barrel alone. (The purpose of segregating the inertia of the barrel from the mounted hardware is to maintain visual validation of the plots; a plot of the combined linear density could obscure the distinction between a valid plot and an erroneous one.) The final plot reveals the axial distribution of cross-sectional stiffness. These input vectors are used to formulate the finite element matrices.

For this model, the barrel is broken up into seven elements to provide ample accuracy of the model in the frequency range of the first few flexible modes. As discussed in Reference [6], the frequency response is greatest in the lowest modes of vibration. This is where the finite element model most accurately mimics the vibration of the underlying distributed parameter system.

To form the finite element mesh, three locations are specified as imposed node locations along the barrel in locations where external constraints may conveniently be incorporated into the dynamic model. The three external constraints are located at the elevation mechanism, the trunnion bearing, and the

vibration absorber (0.540m, 0.988m, and 6.544m, respectively). The absorber is located at the muzzle reference system mount, in order to conveniently test the design concept. In general, the location of the absorber would be a free parameter. The remaining three node locations are placed by the file <fem_mesh.m>. [6] (For seven elements, the beam must be modeled by eight nodes—including the two free ends of the beam, the three imposed node locations, and the three nodes to be placed by the mesh (Figure 2)).

The finite element modeling of the barrel realized by <fem_form.m> [6] results in a 16-by-16 inertial matrix and a cross-sectional stiffness matrix. A damping matrix, which introduces a force opposite in direction and proportional to the velocity of the deformation, is constructed via the Rayleigh proportional damping approximation, as realized by the file <fem_lump.m>. [6] The inertial proportional damping coefficient, α, is set to zero, and the stiffness coefficient, β, is set to set to 0.001 $\frac{N/(m/s)}{N/m}$. (These values are a common approximation for steel structures. Experimental measurements of these values are anticipated for a future report.)

Constraint/Mounting of the Barrel

Once the dynamics of the barrel's distributed parameter system are modeled, they must be constrained by a model of the gun mount. This constraint is applied to the barrel at two locations—the elevation mechanism and the trunnions—and provides constraint forces that are a function of the transverse deflections of the barrel.

Both forces are approximated by a force that is proportional to the lateral deflection of the barrel at the constraint location and opposite in direction (*i.e.*, springs). (For this analysis, both stiffnesses are set to 500,000 $lb_f/in \sim 10^8$ N/m.)

Using arguments developed in Reference [6], the stiffness and damping values of the constraints are added to the respective diagonal elements of the finite element matrices, which correspond to the lateral motion of the constrained node. This implementation is executed by the file <fem_lump.m>.

This parametric formulation of the barrel constraints is limited; the real structure would require more than two values for an accurate model. This approximation results in imprecise boundary conditions on the barrel that have the greatest impact on the lower modes of vibration. However, the model does capture many of the dynamic effects of interest and can easily be modified to incorporate more advanced constraint approximations—including servo-control dynamics.[10]

Coupled External Vibration Absorbers

An interesting dynamic effect can be achieved by coupling an external lumped mass-spring-damper system to structures. This attenuates combined system vibration in

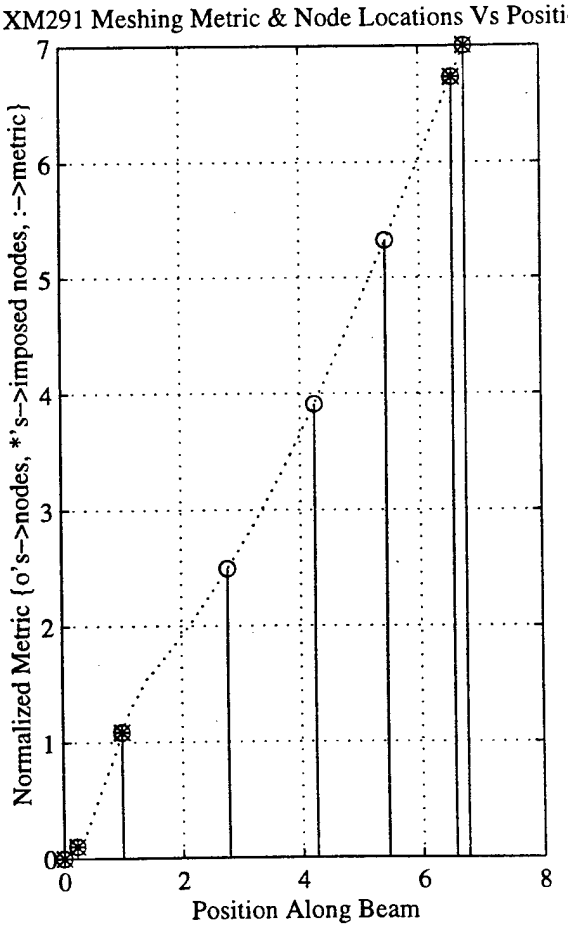

Figure 2. Node placement by meshing metric

a relatively narrow band near the operating frequency of the absorber and dissipates and disperses steady-state energy across a wider band—as long as the damping, stiffness, and inertial coefficients are well-tuned.

With the inclusion of the absorber, a new *energy storing* degree of freedom is added to the total system. This requires a new generalized coordinate to represent the deflection of the absorber—and its time derivatives—from its equilibrium position. This increases the size of the system matrices to 17-by-17 (Figure 3). (The incorporation of the absorber is developed in Reference [6] and implemented by the file <fem_lump.m>.)

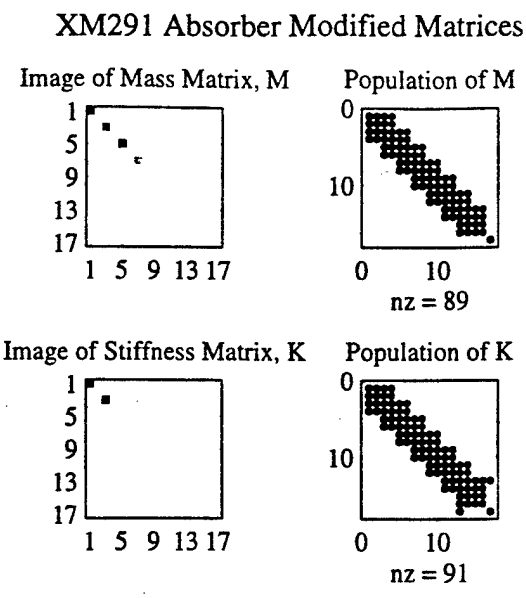

Figure 3. Image of absorber modified system matrices

Figure 3 depicts the completed system mass and stiffness matrices of an absorber modified system. (The absorber stiffness and damping will be optimized later in this report.) The shaded images to the left indicate the relative magnitude of the elements of each matrix. Because the disparity in element magnitude is great, the distinction between small and zero elements may be obscured. To address this issue, the non-zero elements of both matrices, regardless of their magnitude, are revealed to the right (using MATLAB®'s <spy> command [8]). The plots verify the cascading construction of 4-by-4 elemental matrices—resulting in the diagonally banded system matrices for the 16-by-16 finite element portion of the matrices. In addition, the coupling of the absorber to the lateral generalized coordinate (in this case, q_{13}) results in the stiffness elements at $K_{17,13}$, $K_{13,17}$, and $K_{17,17}$. (Interior modification at $K_{13,13}$ is also effected by <fem_lump.m>.) The absorber inertia results in the single element at the lower right-hand corner of the mass matrix, $M_{17,17}$.

Equations of Motion

Once the combined system matrices are formed, the resulting equation of motion is:

$$\boldsymbol{M}\ddot{\underline{q}} + \boldsymbol{C_D}\dot{\underline{q}} + \boldsymbol{K}\underline{q} = \underline{f} \qquad (1)$$

where:

$\boldsymbol{M}$	is the 17-by-17 mass matrix
$\boldsymbol{C_D}$	is the 17-by-17 damping matrix
$\boldsymbol{K}$	is the 17-by-17 stiffness matrix
$\underline{q}$	is the 17-by-1 generalized coordinate vector
$\underline{f}$	is the 17-by-1 generalized force vector
$\cdot$	denotes differentiation with respect to time

In equation (1), M, C_D, and K are the 17-by-17 mass, damping, and stiffness matrices, respectively. The generalized coordinate vector, $\underline{q}$, and force vector, $\underline{f}$, may be related to the nodal displacements and forces as follows:

$$\underline{q} = \begin{bmatrix} q_1 \\ q_2 \\ q_3 \\ q_4 \\ \cdot \\ \cdot \\ \cdot \\ q_{2\times nn-1} \\ q_{2\times nn} \\ q_{2\times nn+1} \end{bmatrix} = \begin{bmatrix} y_1 \\ \theta_1 \\ y_2 \\ \theta_2 \\ \cdot \\ \cdot \\ \cdot \\ y_{nn} \\ \theta_{nn} \\ y_{VA} \end{bmatrix} \quad (a) \qquad \underline{f} = \begin{bmatrix} f_1 \\ f_2 \\ f_3 \\ f_4 \\ \cdot \\ \cdot \\ \cdot \\ f_{2\times nn-1} \\ f_{2\times nn} \\ f_{2\times nn+1} \end{bmatrix} = \begin{bmatrix} F_1 \\ M_1 \\ F_2 \\ M_2 \\ \cdot \\ \cdot \\ \cdot \\ F_{nn} \\ M_{nn} \\ F_{VA} \end{bmatrix} \quad (b) \qquad (2)$$

where:

q_n	is the nth generalized coordinate
f_n	is the nth generalized force
y_n	is the transverse displacement of the nth node
y_{VA}	is the transverse displacement of the absorber
θ_n	is the rotational displacement of the nth node
F_n	is the transverse external force at the nth node
F_{VA}	is the external force applied to the absorber
M_n	is the external applied moment at the nth node
nn	is the total number of nodes

With the exception of gravitational forces, external forces are generally transmitted to the system only through the mount locations (exclusive of the firing event). For example, terrain disturbance forces would be applied to the gun system through the trunnion mounts and *corrected* by the elevation mechanism (f_5 and f_3, respectively). Gravitational forces may be neglected because they result in an equilibrium deflection solution about which the disturbance-induced vibrations will oscillate. This assumption may be compromised if the gun barrel is rapidly elevated—resulting in significant changes of the orientation of the gun relative to the gravity field and subsequent changes in the equilibrium deflection.

Conversion to First-Order State-Space

Many of the powerful MATLAB® tools for dynamic analysis and design require the dynamic equations to be in linear, time-invariant, first-order state-space form. Equation (1) is in the second-order symmetric form. This representation can be converted to the first-order state-space form by using the following method. [6.11]

First, define the state-vector and its first time derivative as the combined generalized coordinates of equation (2) and their first temporal derivatives.

$$\underline{x} = \begin{bmatrix} \underline{q} \\ \dot{\underline{q}} \end{bmatrix} \rightarrow \dot{\underline{x}} = \begin{bmatrix} \dot{\underline{q}} \\ \ddot{\underline{q}} \end{bmatrix} \tag{3}$$

Second, define the system dynamics of equation (1) in terms of the generalized coordinate vector's time derivatives.

$$\begin{aligned} \dot{\underline{q}} &= \boldsymbol{I}\,\dot{\underline{q}} && (a) \\ \ddot{\underline{q}} &= -\boldsymbol{M}^{-1}\boldsymbol{K}\underline{q} - \boldsymbol{M}^{-1}\boldsymbol{C}_D\,\dot{\underline{q}} + \boldsymbol{M}^{-1}\underline{f} && (b) \end{aligned} \tag{4}$$

Note that the form of equation (4) presumes that the mass matrix is invertible. This is always the case for beam finite element formulations. Using equations (3) and (4), a state-space representation with all of the generalized coordinates as the output is as follows:

$$\begin{aligned} \dot{\underline{x}} &= \boldsymbol{A}\underline{x} + \boldsymbol{B}\underline{f} \\ \underline{q} &= \boldsymbol{C}\underline{x} + \boldsymbol{D}\underline{f} \end{aligned} \tag{5}$$

where the state-space matrices are constructed in terms of the second-order system matrices and the zero and identity matrices are of compatible size. (Note that the state-space matrices have twice the number of rows and columns as the second-order system matrices.)

$$\begin{aligned} \boldsymbol{A} &= \begin{bmatrix} \boldsymbol{0} & \boldsymbol{I} \\ -\left(\boldsymbol{M}^{-1}\boldsymbol{K}\right) & -\left(\boldsymbol{M}^{-1}\boldsymbol{C}_D\right) \end{bmatrix} && (a) \qquad \boldsymbol{B} = \begin{bmatrix} \boldsymbol{0} \\ \boldsymbol{M}^{-1} \end{bmatrix} && (b) \\ \boldsymbol{C} &= \begin{bmatrix} \boldsymbol{I} & \boldsymbol{0} \end{bmatrix} && (c) \qquad \boldsymbol{D} = \begin{bmatrix} \boldsymbol{0} \end{bmatrix} && (d) \end{aligned} \tag{6}$$

The m-file <fem2ss.m> [6] computes the state-space matrices using the second-order matrices of equation (1) as shown in equation (6).

FREQUENCY RESPONSE ANALYSIS OF THE MODEL

Model Truncation

Truncation of the state-space model from a multi-input/multi-output system to a single-input/single-output system facilitates frequency response analysis. With this goal in mind, the input and output to be used must be selected. Because terrain disturbances are transmitted to the system via the trunnion mounts, the disturbance forcing is applied at f_5. The *correction force* applied by the elevation mechanism at f_3 is simply modeled as a linear compliance. (Inclusion of the fire-control dynamics, as previously done by Dholiwar [10], would enhance the model significantly and will be pursued in the future.) The muzzle pointing angle is selected as the sole output of the system because it includes contributions

from all vibratory modes. (The muzzle is an *anti*-node of the constrained beam.) The truncation is effected by the <ssselect> command [9], as demonstrated in Reference [6].

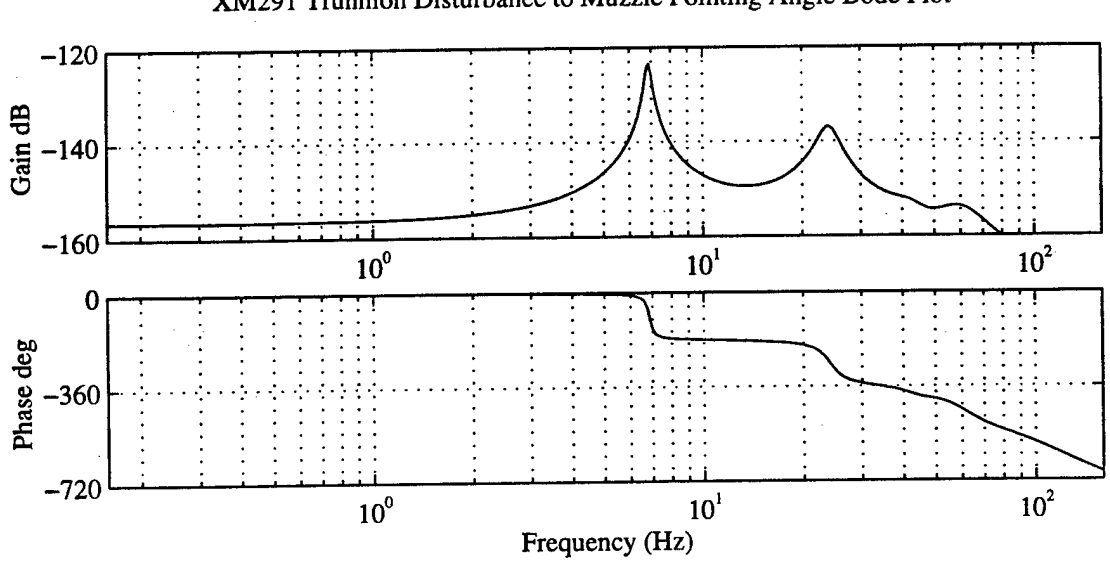

Figure 4. Base-line Bode plot of unmodified XM291 gun system

Bode Analysis of Unmodified Barrel

Once single-input/single-output state-space is realized, the frequency response of the system can be computed using the <bode> command. [9] Think of this as a cross-section of the Laplace transfer function along the imaginary frequency axis by substituting jω for "*s*," where ω is the radial frequency. The frequency response of a dynamic system indicates the steady-state response, $y(t)$, of the system to a sinusoidal input, $u(t)$: [9]

$$\begin{aligned} u(t) &= A\sin\left((2\pi f)t\right) \\ y(t) &= kA\sin\left((2\pi f)t + \phi\right) \end{aligned} \tag{7}$$

where:

$u(t)$	is the input force at the trunnions
A	is the amplitude of the input force
f	is the cyclic frequency of the input force
t	is time
$y(t)$	is the output pointing angle of the muzzle
k	is the gain
ϕ	is the phase lead/lag of the response.

Figure 4 is a Bode plot of the response of the muzzle pointing angle to disturbance trunnion loading of the unmodified barrel. Use this as a baseline for judging modified barrels. It consists of two plots. The upper plot relates the gain of the system, k in equation (7), to the excitation frequency, f. The

lower plot depicts the phase lag, ϕ, to the frequency. The gain is represented in decibels. (A decibel is related to the gain as: dB = 20 $\log_{10}(k)$.)

FREQUENCY DOMAIN OPTIMIZATION OF THE ABSORBER

Bode Analysis for Absorber Optimization

The frequency response of a modified barrel is affected in the same manner as the unmodified barrel. For this paper, two absorber parameters are varied—the stiffness, K_{VA}, and the stiffness proportional damping coefficient, β_{VA}—while the mass of the absorber, M_{VA}, is maintained at 20 Kg. The gain function of the modified barrel is then divided by the gain of the original system—resulting in a relative frequency response (Figure 5).

A weighting function is then applied to emphasize the response in the frequency range of primary interest. This function (Figure 6) was generated as the normalized response of a second-order system with natural frequency, f_n, of 9 Hz and a critical damping ratio, ζ, of 40%. In general, the weighting function effectively combines the dynamics of the gun system with a priori knowledge of the frequency content of the disturbance force. (Multiplication in the frequency domain is equivalent to convolution in the time domain. [12]) Thus, this weighting function approximates *white* terrain-induced trunnion disturbances as having been passed through a second-order, damped filter.

A single scalar cost function, J, is then quantitatively computed across the frequency range of interest as the integral of the weighted relative frequency response of the absorber modified system.

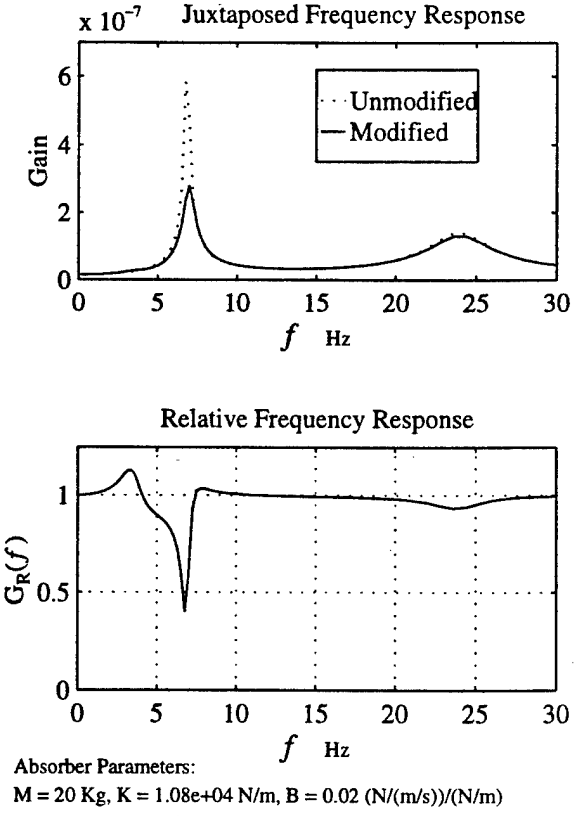

Figure 5. Juxtaposition of modified and unmodified barrels and the resulting relative frequency response

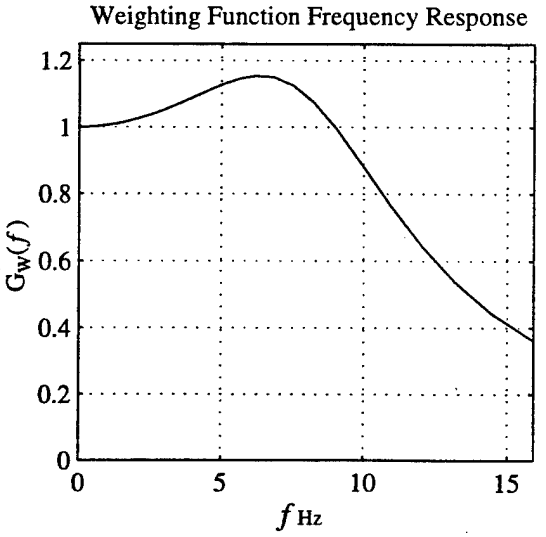

Figure 6. Weighting function used to emphasize expected disturbance frequency content in the optimization

$$J = \int_{f_{low}}^{f_{high}} \left(G_R(f) G_W(f) \right) df \tag{8}$$

where:

J	is the scalar cost function
f_{low}	is the lowest frequency of interest
f_{high}	is the highest frequency of interest
$G_R(f)$	is the relative frequency response as shown in Figure 5
$G_W(f)$	is the weighting function frequency response as shown in Figure 6

J is subsequently normalized to be unity for K_{VA} and β_{VA} at zero; these values essentially eliminate the effects of the absorber. Other cost functions can be used to incorporate other design considerations (such as worst-case performance) or pragmatic engineering issues (such as bounds on reasonable damping levels). Strategic formulation of the cost function is more of a concern when the dimension of the parametric design space increases—thus requiring all multi-dimensional gradient descent methods for optimization such as the <fmin> command. [8] For the two-dimensional case at hand, visual inspection of the optimization surface, $J(\beta_{VA}, K_{VA})$, is possible.

RESULTS

Optimization Surface

The optimization surface generated for a 20 Kg vibration absorber using the scalar frequency response cost function is shown in Figure 7.

The plots clearly indicate that, for low levels of damping, $\beta \leq 0.005$s, the absorber design is extremely sensitive to parametric variation. This can be seen by the high density of contour lines near the peaks that indicate step gradients.

The peaks are caused by detrimental interaction of the absorber with the fundamental frequencies of the barrel. As mentioned earlier, this implies that low-level damping absorber designs are sensitive to model uncertainty caused by the unmodeled mount and elevation servo-control dynamics. That said, the contour plot indicates that at least one low-level damping design, near $K_{VA} = 10{,}000$ N/m, would effect disturbance rejection by the absorber.

Optimization Surface in Parameter Space

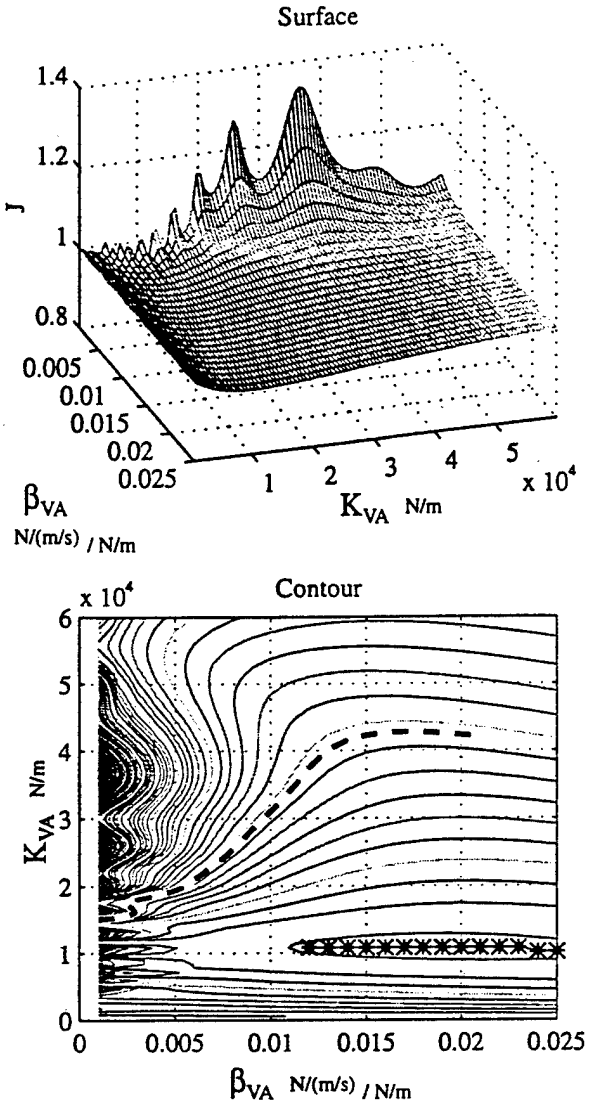

Figure 7. The optimization surface of a 20 Kg absorber

The top plot depicts a 3D rendering of the surface. The bottom plot reveals a contour of the surface. The dashed line represents the unity J value. The asterisks represent optimal parameter values that minimize J.

For higher damping levels, (*i.e., 0.005s* $\leq \beta_{VA} <$ *0.030s*), the absorber design appears to be quite insensitive, especially to the level of damping.

In both cases, the lack of sensitivity to damping levels is a desirable result. Engineering obstacles with damping materials that are subject to harsh variations in temperature—as would be experienced in a weapons environment—may be relaxed because of this lack of sensitivity.

Relative Frequency Response

Figure 7 demonstrates that the optimal "spring-constant" of 11,400 N/m that couples the 20 Kg absorber to the gun barrel is essentially constant for the range of β_{VA}'s examined. (Actually, for the low damping values, the optimization bifurcates with a slight advantage for a K_{VA} of 9,600 N/m.)

Figure 8 depicts the change in the frequency response gain due to an optimal absorber for various Rayleigh damping values. The "*spikes*" in the response for low damping may be offset by the deep "*notch-filter*" effect these systems exhibit. If modeling uncertainty is very low, matching the notch-filter to known problem disturbances may be a viable design method.

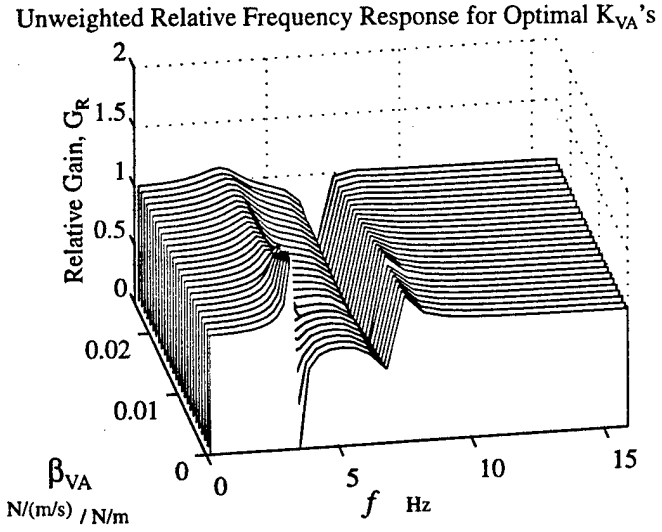

Figure 8. Relative frequency response of a 20 Kg absorber for optimal K_{VA}'s (~10,000 N/m) versus Rayleigh damping β_{VA}'s

For the case at hand, the "*notch-filter*" approach is viable if:

i. Prototype hardware *tuning* of the parameters to match the real system is possible.
ii. Interaction with the fire-control servo loop is well-modeled.
iii. Modal interaction with other unmodeled structures (such as the turret) does not coincide with the absorber *"spikes."*

The advantages of a design with significant damping levels are clearly based on a lack of model and structural sensitivity. Unless there is an *absolute* need for a "*notch-filter*" level of disturbance rejection, this robust behavior is the preferred design approach.

Pole-Zero Plots in the Laplace Domain

The location of the damped eigenvalues and zeros in the Laplace domain provides insight into the dynamics of the absorber modified gun system.

Often called a pole-zero map, the unmodified system is shown in Figure 9. In this figure, the first four bending modes are revealed as the complex conjugate "x" pairs. The natural coordinate units for the imaginary axis are radians per time, but this axis is scaled to display the more familiar cyclic Hertz (Hz) frequency.

The polar grid correlates damped frequencies to their natural (undamped) counterparts by the arcs of constant radius.

The critical damping ratio, ζ, for each mode is revealed by the angular displacement off the imaginary axis. Each radial line represents a 20% increment of the critical damping—from zero at the imaginary axis to 100% along the real axis.

It is important to realize that roots in this domain imply that the denominator of the transfer function goes to zero as these roots are approached. This leads to unbounded response at these locations; thus the term "pole."

Conversely, the zeros of the transfer function are depicted by the "o" marks. At these locations, the transfer function numerator is zero, which nullifies any response from the system at these locations.

The effect of these values on the frequency response occurs along the imaginary axis—where the real parts of the Laplace domain "s" variables are zero. As a surface, the transfer function along the imaginary axis closely mimics the response of the poles and the zeros near it. Thus, in Figure 9, the nearby location of the eigenvalue located at 6.8 Hz effects a spike in the frequency response function (as seen in Figures 4 and 5). Because the pole does not coincide with the imaginary axis, the spike is not unbound, as would be expected in an undamped model.

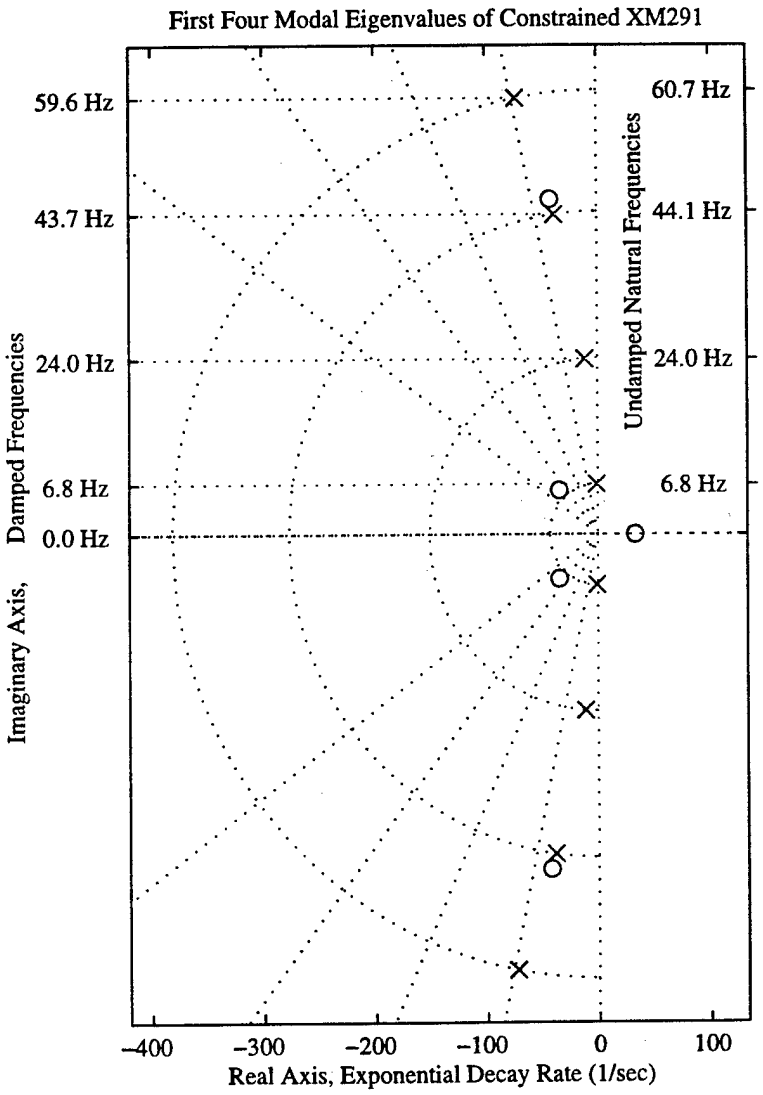

Figure 9. Pole-zero plot in Laplace domain of unmodified gun system

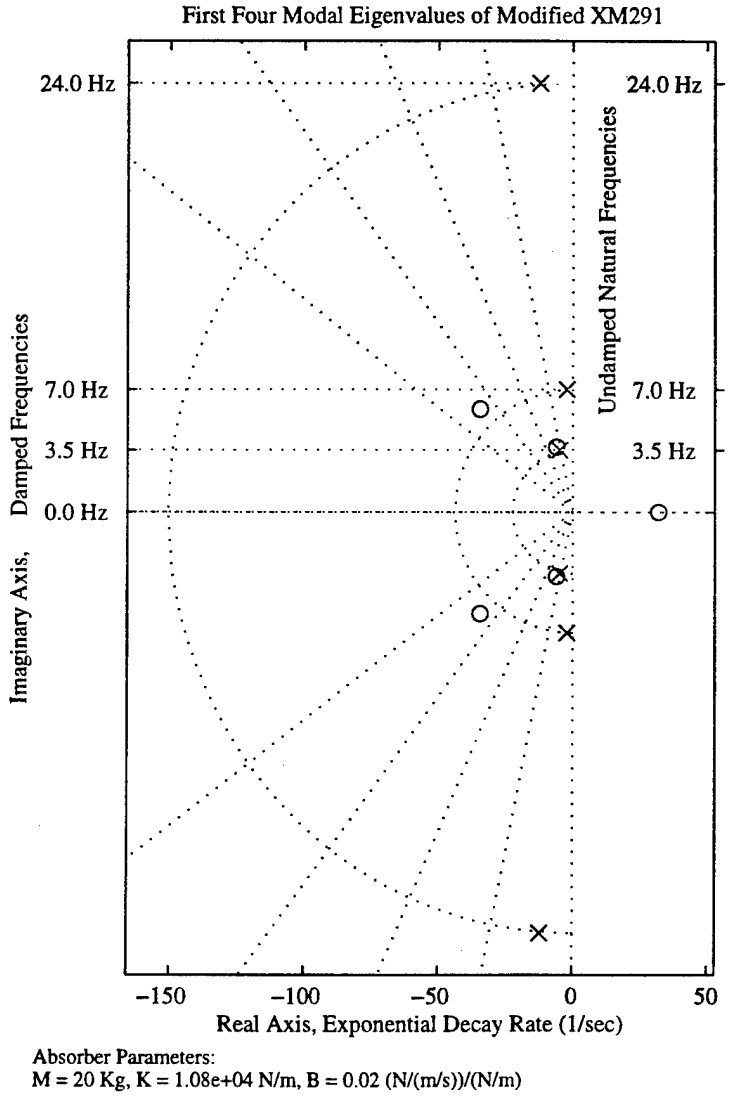

Figure 10. The pole-zero map of the gun modified by an optimal 20 Kg absorber

The absorber changes the pole-zero map by introducing a new degree of freedom and its subsequent poles and zeros.

Figure 10 depicts the new pole-zero map of the modified gun system. The 20 Kg absorber has created a pair of conjugate poles and zeros, and the optimization has placed the new zeros very near to the new poles—with a slight translation to a higher frequency.

The absorber pole location almost coincides with the natural frequency the absorber would exhibit if it were constrained to a rigid reference. This natural frequency can be evaluated as $\omega_n = \sqrt{(K_{VA}/M_{VA})}$. Divided by 2π radians per cycle, this value is 3.70 Hz for the absorber parameters M_{VA} = 20 Kg and K_{VA} = 10,800 N/m. Located near 3.5 Hz, the absorber pole is below the rigid coupling value because of the relatively high barrel contribution to its effective inertia (as opposed to stiffness) and the modest level of damping.

The close proximity of the zero to the pole largely cancels the response of the pole. However, because the zero is shifted higher, the pole does effect a small increase in response toward the low-frequency side. This effect is readily seen in Figures 5 and 8.

The zero subsequently reduces the response of the system toward the higher frequencies, especially the next pole. The effect diminishes as the input disturbance frequency moves up the imaginary axis.

In addition, the coupling of the absorber has slightly increased the effective stiffness of the original first mode of the gun system. This is seen as the shift of the 6.8 Hz pole in Figure 9 to 7.0 Hz in Figure 10.

For an absorber designed with low damping, the new pole-zero pair becomes nearly collocated with the imaginary axis—resulting in the pronounced spike and notch effects in Figure 8.

Mode Shape Comparison

The mode shapes (eigenvectors) of both the original and the 20 Kg absorber modified barrels were evaluated (Figures 11 and 12) using the <eigen_2o.m> file developed in Reference [6]. In both cases, the mode shapes are mass-normalized.

The x's along the barrel center line indicate the node locations. The external coupling at the elevation mechanism and the trunnions is shown by the small circle around the x. The absorber deflection in Figure 12 is depicted by the circle—constrained to the barrel—by the thin line.

Figure 12 depicts the nearly decoupled first mode of the vibration absorber. (The flexure of the barrel in this mode shape is nearly rigid body.) Although the rather large deflection of the absorber in the first mode would normally cause concern, the near *pole-zero cancellation* shown in Figure 10 largely alleviates this problem. The first mode essentially coincides with the notch depicted in Figures 5 and 8.

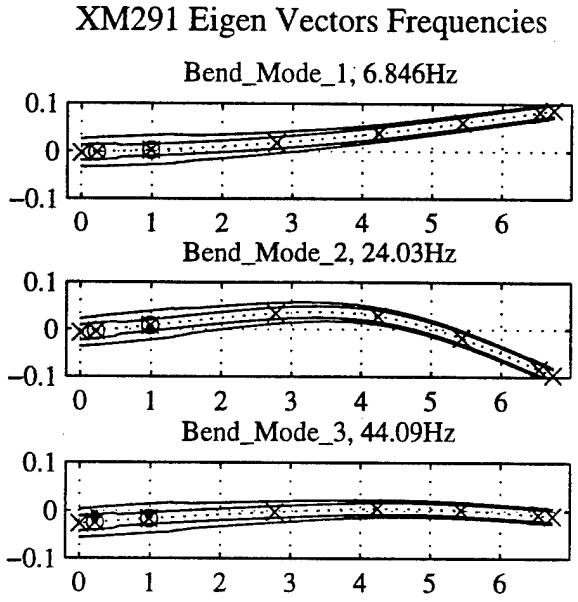

Figure 11. First three mode shapes and frequencies of the unmodified gun system

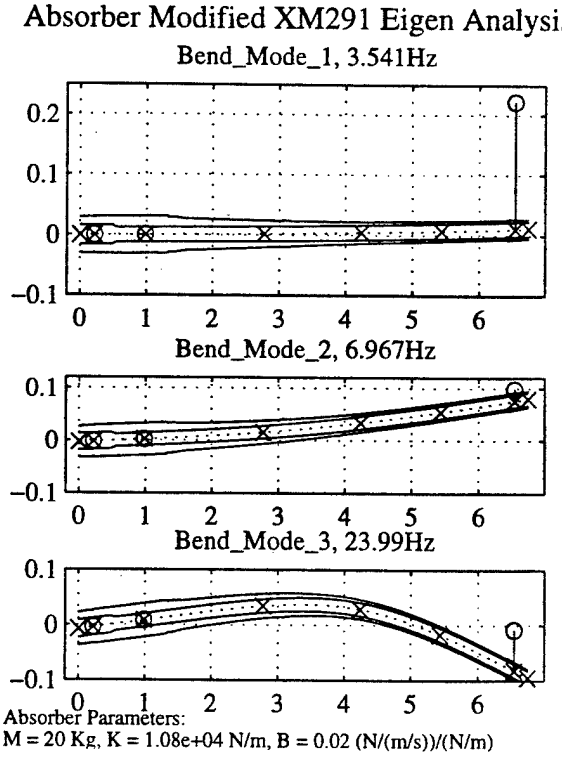

Figure 12. First three mode shapes and frequencies of the gun system modified by an optimal absorber

CONCLUSIONS

Vibration absorbers present an opportunity to reduce the receptance of gun systems to terrain-induced vibrations by using a simple passive mechanism. The design method presented in this paper optimizes the design and reveals the sensitivity of the design to the parametric uncertainty of the absorber—as revealed by the gradient of the optimization surface. Optimization within a high dimensional parameter space was enabled by the identification of a scalar cost-function in the frequency domain of the system, which is readily computed with MATLAB® software. This cost function may be adapted to disturbances characterized a priori via a weighting function in the frequency domain. This weighting in the frequency domain is equivalent to convolution in the time domain of the gun system with the approximated disturbance system.

Absorber performance was evaluated in the Laplace domain using pole-zero plots, frequency domain via Bode analysis, and eigen techniques. This verified the advantages of designing an absorber with significant damping levels, which helps to avoid undue sensitivity to modeling and parametric uncertainties.

The sensitivity of designs that are low in damping—to slight parametric variations, model uncertainty, and unmodeled dynamics—were shown. In addition, the potential advantage of the "notch-filter" effect was demonstrated in case the disturbance can accurately be characterized a priori; this justifies significant modeling and validation efforts to reduce the potentially detrimental uncertainties. Terrain-induced vibrations are unlikely to be well-characterized; however, undesirable servo-control dynamics may provide a candidate for this type of approach.

REFERENCES

1. Thomson, W. T., *Theory of Vibration with Applications, 4th ed.* Prentice Hall, Englewood Cliffs, NJ, 1993.

2. Timoshenko, S., and Young, D.H., *Vibration Problems in Engineering, 3rd ed.,* D. Van Nostrand Company, Inc., New York, NY, 1955.

3. Crede, C.E., *Shock and Vibration Engineering Concepts in Engineering Design*, Prentice-Hall, Englewood Cliffs, NJ, 1965.

4. Leipolz, H. H. E. and Abdel-Rohman, M., *Control of Structures,* Martinus Nijhoff Publishers, Boston, MA, 1986.

5. Rofooei, F. R., "Active Control of Structures," Ph.D. Thesis, Rensselaer Polytechnic Institute, Troy, NY, May 1992.

6. Kathe, E., "MATLAB® Modeling of Non-Uniform Beams Using the Finite Element Method for Dynamic Design and Analysis," ARDEC Technical Report ARCCB-TR-96010, Benet Laboratories, Watervliet, NY, April 1996.

7. *MATLAB® User's Guide*, The MathWorks, Inc., Natick, MA, July 1993.

8. *MATLAB® Reference Guide*, The MathWorks, Inc., Natick, MA, July 1993.

9. *Control System Toolbox User's Guide*, The MathWorks, Inc., Natick, MA, June 1994.

10. Dholiwar, D. K., "Development of a Hybrid Distributed-Lumped Parameter Openloop Model of Elevation Axis for a Gun System," Proceedings of the Seventh U.S. Army Symposium on Gun Dynamics, ARCCB-SP-93034, Benet Laboratories, Watervliet, NY, 11-13 May 1993, pp. 368-385.

11. Meirovitch, L., *Dynamics and Control of Structures*, John Wiley & Sons, New York, NY, 1990.

12. Bracewell, Ronald N., *The Fourier Transform and Its Application, 2nd ed. (revised)*, McGraw-Hill, New York, NY, 1986.

TECHNICAL REPORT INTERNAL DISTRIBUTION LIST

	NO. OF COPIES
CHIEF, DEVELOPMENT ENGINEERING DIVISION	
ATTN: AMSTA-AR-CCB-DA	1
-DB	1
-DC	1
-DD	1
-DE	1
CHIEF, ENGINEERING DIVISION	
ATTN: AMSTA-AR-CCB-E	1
-EA	1
-EB	1
-EC	1
CHIEF, TECHNOLOGY DIVISION	
ATTN: AMSTA-AR-CCB-T	2
-TA	1
-TB	1
-TC	1
TECHNICAL LIBRARY	
ATTN: AMSTA-AR-CCB-O	5
TECHNICAL PUBLICATIONS & EDITING SECTION	
ATTN: AMSTA-AR-CCB-O	3
OPERATIONS DIRECTORATE	
ATTN: SIOWV-ODP-P	1
DIRECTOR, PROCUREMENT & CONTRACTING DIRECTORATE	
ATTN: SIOWV-PP	1
DIRECTOR, PRODUCT ASSURANCE & TEST DIRECTORATE	
ATTN: SIOWV-QA	1

NOTE: PLEASE NOTIFY DIRECTOR, BENÉT LABORATORIES, ATTN: AMSTA-AR-CCB-O OF ADDRESS CHANGES.

TECHNICAL REPORT EXTERNAL DISTRIBUTION LIST

	NO. OF COPIES
ASST SEC OF THE ARMY RESEARCH AND DEVELOPMENT ATTN: DEPT FOR SCI AND TECH THE PENTAGON WASHINGTON, D.C. 20310-0103	1
DEFENSE TECHNICAL INFO CENTER ATTN: DTIC-OCP (ACQUISITIONS) 8725 JOHN J. KINGMAN ROAD STE 0944 FT. BELVOIR, VA 22060-6218	2
COMMANDER U.S. ARMY ARDEC ATTN: AMSTA-AR-AEE, BLDG. 3022	1
AMSTA-AR-AES, BLDG. 321	1
AMSTA-AR-AET-O, BLDG. 183	1
AMSTA-AR-FSA, BLDG. 354	1
AMSTA-AR-FSM-E	1
AMSTA-AR-FSS-D, BLDG. 94	1
AMSTA-AR-IMC, BLDG. 59 PICATINNY ARSENAL, NJ 07806-5000	2
DIRECTOR U.S. ARMY RESEARCH LABORATORY ATTN: AMSRL-DD-T, BLDG. 305 ABERDEEN PROVING GROUND, MD 21005-5066	1
DIRECTOR U.S. ARMY RESEARCH LABORATORY ATTN: AMSRL-WT-PD (DR. B. BURNS) ABERDEEN PROVING GROUND, MD 21005-5066	1
COMMANDER ROCK ISLAND ARSENAL ATTN: SMCRI-SEM ROCK ISLAND, IL 61299-5001	1
COMMANDER U.S. ARMY TANK-AUTMV R&D COMMAND ATTN: AMSTA-DDL (TECH LIBRARY) WARREN, MI 48397-5000	1
COMMANDER U.S. MILITARY ACADEMY ATTN: DEPARTMENT OF MECHANICS WEST POINT, NY 10966-1792	1
U.S. ARMY MISSILE COMMAND REDSTONE SCIENTIFIC INFO CENTER ATTN: AMSMI-RD-CS-R/DOCUMENTS BLDG. 4484 REDSTONE ARSENAL, AL 35898-5241	2
COMMANDER U.S. ARMY FOREIGN SCI & TECH CENTER ATTN: DRXST-SD 220 7TH STREET, N.E. CHARLOTTESVILLE, VA 22901	1
COMMANDER U.S. ARMY LABCOM, ISA ATTN: SLCIS-IM-TL 2800 POWER MILL ROAD ADELPHI, MD 20783-1145	1

NOTE: PLEASE NOTIFY COMMANDER, ARMAMENT RESEARCH, DEVELOPMENT, AND ENGINEERING CENTER, BENÉT LABORATORIES, CCAC, U.S. ARMY TANK-AUTOMOTIVE AND ARMAMENTS COMMAND, AMSTA-AR-CCB-O, WATERVLIET, NY 12189-4050 OF ADDRESS CHANGES.

TECHNICAL REPORT EXTERNAL DISTRIBUTION LIST (CONT'D)

	NO. OF COPIES
COMMANDER U.S. ARMY RESEARCH OFFICE ATTN: CHIEF, IPO P.O. BOX 12211 RESEARCH TRIANGLE PARK, NC 27709-2211	1
DIRECTOR U.S. NAVAL RESEARCH LABORATORY ATTN: MATERIALS SCI & TECH DIV WASHINGTON, D.C. 20375	1
WRIGHT LABORATORY ARMAMENT DIRECTORATE ATTN: WL/MNM EGLIN AFB, FL 32542-6810	1
WRIGHT LABORATORY ARMAMENT DIRECTORATE ATTN: WL/MNMF EGLIN AFB, FL 32542-6810	1

NOTE: PLEASE NOTIFY COMMANDER, ARMAMENT RESEARCH, DEVELOPMENT, AND ENGINEERING CENTER, BENÉT LABORATORIES, CCAC, U.S. ARMY TANK-AUTOMOTIVE AND ARMAMENTS COMMAND, AMSTA-AR-CCB-O, WATERVLIET, NY 12189-4050 OF ADDRESS CHANGES.

DEPARTMENT OF THE ARMY
ARMAMENT RESEARCH, DEVELOPMENT AND ENGINEERING CENTER
BENÉT LABORATORIES, CCAC
US ARMY TANK-AUTOMOTIVE AND ARMAMENTS COMMAND
WATERVLIET, N.Y. 12189-4050

OFFICIAL BUSINESS
AMSTA-AR-CCB-O
TECHNICAL LIBRARY

DA Label 18-1, Sep 83
Edition of Oct 74 will be used until exhausted.

DEPARTMENT OF THE ARMY

OFFICIAL BUSINESS

Defense Technical Information Center
Attn: DTIC-OCP (Acquisitions)
8725 John J. Kingman Road
Ste 0944
Ft. Belvoir, VA 22060-6218